This article has been accepted for publication in a future issue of this journal, but has not been fully edited. Content may change prior to final publication. Citation information: DOI 10.1109/TVT.2014.2305978, IEEE Transactions on Vehicular Technology

Group Testing Based Spectrum Hole Search for Cognitive Radios

Abhay Sharma and Chandra R. Murthy *Senior Member, IEEE*

***Abstract*—This paper investigates the use of adaptive group testing for finding a spectrum hole of a specified bandwidth in a given wideband of interest. We propose a group testing based spectrum hole search algorithm that exploits sparsity in the primary spectral occupancy by testing a group of adjacent sub-bands in a single test. This is enabled by a simple and easily implementable sub-Nyquist sampling scheme for signal acquisition by the cognitive radios. The sampling scheme deliberately introduces aliasing during signal acquisition, resulting in a signal that is the sum of signals from adjacent sub-bands. Energy-based hypothesis tests are used to provide an occupancy decision over the group of sub-bands, and this forms the basis of the proposed algorithm to find contiguous spectrum holes of a specified bandwidth. We extend this framework to a multi-stage sensing algorithm that can be employed in a variety of spectrum sensing scenarios, including non-contiguous spectrum hole search. Further, we provide the analytical means to optimize the group tests with respect to the detection thresholds, number of samples, group size, and number of stages, to minimize the detection delay under a given error probability constraint. Our analysis allows one to identify the sparsity and SNR regimes where group testing can lead to significantly lower detection delays compared to a conventional bin-by-bin energy detection scheme; the latter is in fact a special case of the group test when the group size is set to 1 bin. We validate our analytical results via Monte Carlo simulations.**

***Index Terms*—Group testing, spectrum hole search, sub-Nyquist sampling, energy detection, multi-stage sensing, frequency hopping.**

I. Introduction

Group testing is a natural framework for efficiently identifying the defective items in a large population containing a small fraction of defective items [2]. It is applicable in scenarios where multiple items can be tested together in a single test; the group test returns positive if at least one item in the group is defective, and returns negative otherwise. Group tests are particularly useful when individually testing each item is prohibitively time-consuming, since testing multiple items in a single test leads to time savings when test outcomes are negative. One area where group tests could potentially offer significant benefits is that of spectrum hole search for Cognitive Radio (CR) [3]–[5]. The CR paradigm is based on the fact that, at any given time, the spectral occupancy by the primary users is sparse over a wideband of interest [6], [7]. For efficient functioning, CR networks need accurate and up-to-date information about the availability of spectrum holes, i.e., frequency bands where the primary users are inactive.

In this work, we focus on the application of *adaptive* group testing to the task of finding *a* spectrum hole of a pre-specified bandwidth within a given wideband of interest for use by the CR network. This problem is relevant in many CR scenarios. For example, in the IEEE 802.22 standard for cognitive radio, the primary users occupy a bandwidth of 6 MHz each. A secondary network that requires 40 MHz of bandwidth for its operation will need to find a spectrum hole consisting of 7 contiguous unoccupied bands. In practice, it is desirable to have the CR network operate in a contiguous frequency band, as this simplifies transceiver hardware design and helps improve the energy efficiency of the CR network compared to using non-contiguous frequency bins. Other considerations for preferring contiguous frequency bin allocation are the physical layer access mechanism (e.g., code division multiple access), network quality of service requirements, spectral mask constraints, etc.

We consider a setup where a CR wishes to identify a given number, say N_e, contiguous unoccupied sub-bands over a given wide bandwidth. A straightforward approach to this problem would be to test each sub-band sequentially, one at a time, till the required N_e contiguous bins are found. On the other hand, group testing can be used to reduce the search time in such a problem, if a set of adjacent sub-bands can be tested at one shot. One way to accomplish this without increasing the sampling rate and processing requirements at the CR node is to acquire the analog signal corresponding to $M(\geq 1)$ sub-bands using a wide front-end anti-aliasing filter, followed by sampling at a rate corresponding to the Nyquist rate for a *single* sub-band. Although sampling at the Nyquist rate of a single sub-band results in aliasing, it provides the receiver with a signal that is the *sum of the signals in all the acquired sub-bands.* Based on the energy of the aliased signal, in this paper, we develop an energy-based detector, referred to as *an M-bin group test*, to provide a joint occupancy decision on the group of M adjacent sub-bands over which the signal is acquired. We consider the popular energy-based detection (see [8]–[10] for an excellent survey of spectrum sensing), as it is easy to implement and is optimal when the CR has no prior information about the primary signal [11].

In the literature, the idea of sampling the signal over multiple sub-bands and make joint occupancy decisions has been explored, but with sampling at the Nyquist rate corresponding to the multiple sub-bands. For example, FFT-based architectures that collect samples at a Nyquist rate corresponding to C_N narrowbands and can provide simultaneous decisions for all the C_N bins have been considered [12]–[14]. A two-stage sensing architecture that reduces search times by extending the narrowband energy detector to wider bands has been

The authors are with the Dept. of Electrical Communication Engg. at IISc, Bangalore, India. (e-mails: abhay.bits@gmail.com, cmurthy@ece.iisc.ernet.in)

This work was financially supported by a research grant funded by the directorate of extramural research and intellectual property rights, DRDO, Govt. of India.

This work has appeared in part in [1].

This article has been accepted for publication in a future issue of this journal, but has not been fully edited. Content may change prior to final publication. Citation information: DOI 10.1109/TVT.2014.2305978, IEEE Transactions on Vehicular Technology

proposed in [15]. Another way to reduce the search time is by employing parallel data chains, e.g., using multiple antenna receivers [16], [17]. However, the effective sampling rate requirements of these architectures are higher than the narrowband detector, since data is acquired over multiple narrowbands at Nyquist rates. Increasing the sampling rate entails higher power consumption and processing requirements, which is undesirable in tasks such as spectrum sensing, which are frequently performed at the CR nodes. A wideband sensing framework is proposed in [18], [19], where a bank of multiple narrowband energy detectors operating at Nyquist sampling rate are jointly optimized by choosing different thresholds, to maximize the total opportunistic CR throughput, while constraining the interference to the primary users. The above framework requires the knowledge of primary-to-secondary channel coefficients and secondary throughput values for each narrowband, and is therefore limited to scenarios where such information is available. In practice, it may be hard for the CR to obtain or estimate these parameters.

Group testing based signal acquisition leads to noise enhancement (folding), due to the aliasing introduced by the sub-Nyquist sampling. This phenomenon is also seen in other wideband acquisition systems operating at sub-Nyquist rates, such as compressive sensing based methods [20]. This raises important questions about the efficacy of group testing in the face of noise folding, and the dependence of the optimal test parameters on the operating SNR and the sparsity in the frequency occupancy of primary users. In this context, our contributions in this paper are as follows:

1) We introduce a signal acquisition scheme that enables the use of group testing based spectrum hole search by acquiring wideband signals at a fixed sampling rate. The acquisition scheme entails only a minimal hardware change, compared to the narrowband energy detector, in the form of a programmable anti-aliasing filter (See Sec. II).
2) We present a search algorithm that minimizes the time to detect a spectrum hole of a specified bandwidth while satisfying an upper bound on the probability of incorrectly identifying the hole (See Sec. III).
3) We theoretically analyze the detection delay behavior of the algorithm, and use it to optimize the parameters (group size, samples per test, and detection thresholds) of the search algorithm. We also identify the regimes of the sparsity and detection SNR where group tests offer performance benefits over the conventional bin-by-bin search scheme. In particular, our analytical characterization of the detection delay of the bin-by-bin detector is also new (See Sec. IV).
4) We present a multi-stage detection algorithm that combines multiple group sizes to identify a large fraction of the available spectrum holes as fast as possible (See Sec. V).

Extensive simulation results corroborate our theoretical analysis and illustrate the performance benefits obtainable from the group testing approach under favorable conditions on sparsity and SNR (See Sec. VI). The use of group tests with the optimal group size leads to a faster acquisition of the desired spectrum hole. This, in turn, leads to a better utilization of the available spectrum, since a shorter sensing duration leaves more time for data transmission. Reducing the sensing duration is also power efficient, since spectrum sensing is a frequently-running task on CR devices. Moreover, group test based schemes significantly reduce the total number of tests that need to be set up while searching over a given wideband, thereby reducing the test setup overheads [15]. Finally, we note that the spectrum hole search algorithm always selects the optimal group size M. In particular, in scenarios where $M = 1$ is optimal, the group testing scheme reduces to the conventional bin-by-bin search scheme.

Notation: $\mathcal{N}(m, s^2)$ represents the Gaussian distribution with mean m and variance s^2. $\chi^2(n)$ denotes Chi-squared distribution with n degrees of freedom. $Q(.)$ denotes the standard Gaussian tail function and $sgn(.)$ denotes the signum function. $Pr\{A\}$ denotes the probability of occurrence of an event A and $Pr\{A|B\}$ denotes the conditional probability of occurrence of event A given event B.

II. Signal Acquisition Scheme

We model the wideband as a set of consecutive non-overlapping frequency narrowbands. Let f_b denote the bandwidth of a narrowband channel, also referred to as a bin or a sub-band. Let the wideband being searched consist of N contiguous sub-bands. Let $S_l(\jmath\Omega)$ and $s_l(t)$ represent the frequency domain and time domain signal components in the l^{th} bin, respectively, down converted to the baseband (denoted $s_l(t) \overset{\mathcal{F}}{\longleftrightarrow} S_l(\jmath\Omega)$). Let $\Omega \triangleq 2\pi f$. By our assumption on the bandwidth of each bin, we have $S_l(\jmath\Omega) = 0, |\Omega| > 2\pi f_b/2$. The frequency domain signal for the wideband channel, down converted to the baseband, can be represented as

$$X(\jmath\Omega) = \sum_{l=-(N-1)/2}^{(N-1)/2} S_l\left(\jmath\Omega - \jmath\Omega_l\right) \tag{1}$$

where $\Omega_l \triangleq 2\pi l f_b$ represents the center frequency of the l^{th} bin. In the above, N is assumed to be odd, but the extension to even N is straightforward.

We now describe a signal acquisition scheme that enables group testing of multiple adjacent bins without increasing the sampling rate requirements at the CR node. Let M denote the number of adjacent bins over which the signal is acquired. The incoming down-converted signal is first passed through an anti-aliasing filter of bandwidth Mf_b to eliminate the out-of-band signals and noise. The frequency domain signal at the output of the anti-aliasing filter can be represented as

$$X_a(\jmath\Omega) = \sum_{l=-(M-1)/2}^{(M-1)/2} S_l\left(\jmath\Omega - \jmath\Omega_l\right). \tag{2}$$

The signal $x_a(t) \overset{\mathcal{F}}{\longleftrightarrow} X_a(\jmath\Omega)$ is sampled at a rate $f_s = f_b$. Since the anti-aliasing filter band-limits the signal to $[-Mf_b/2,\ Mf_b/2]$, sampling at a rate f_b introduces *aliasing*. Let $T_b = 1/f_b$. Let $x_d[n] = x_a(nT_b)$ represent the sampled signal and $x_d[n] \overset{\mathcal{F}}{\longleftrightarrow} X_d(e^{\jmath\omega})$, where $\omega = 2\pi f/f_b$

This article has been accepted for publication in a future issue of this journal, but has not been fully edited. Content may change prior to final publication. Citation information: DOI 10.1109/TVT.2014.2305978, IEEE Transactions on Vehicular Technology

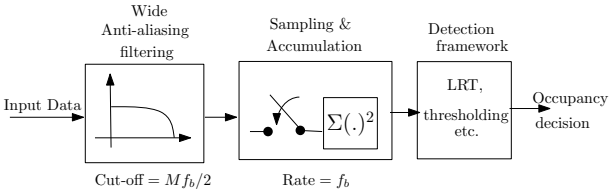

Fig. 1. Block diagram of the wideband signal acquisition system.

[21]. With the above notation, for odd M, $X_d(e^{\jmath\omega}) = (1/T_b)\sum_{l=-(M-1)/2}^{(M-1)/2} S_l\left(\jmath\omega/T_b\right)$. Again, the extension to even M is straightforward. The received signal, $x_d[n]$, is thus the sum of the signal components in the individual bins. Now, the received signal $y_g[n]$ can be described by

$$y_g[n] = x_d[n] + v_g[n] \tag{3}$$

where $v_g[n]$ is the white noise component after aliasing.

Now, due to possibly independent fading across the bins and mismatches between transmit and receive pulse shaping filters, timing and frequency offsets, etc. between the primary transmitter and the CR receivers, the signals from different bins are effectively the result of passing a random signal through orthogonal filters, since the different frequency bins are non-overlapping. Hence, it is reasonable to model the signal contributions from different bins as being mutually independent. Since we assume no knowledge about the primary signal characteristics at the secondary node, we model the signal contributions from l^{th} bin as Gaussian distributed with zero mean and variance P_l, as in [14], [22], [23]. We assume that the baseband signal is real-valued for simplicity of exposition; the extension to complex signals is immediate. We note that, $v_g[n] \sim \mathcal{N}\left(0, M\sigma^2\right)$, where $\sigma^2 = N_o f_b$, and N_o is the white noise power spectral density. The factor M in the noise variance is due to the aliasing introduced by sampling at rate f_b. We accumulate the energy from K samples at the output of the filter, and compute the following test statistic:

$$T(y) = \sqrt{\sum_{n=1}^{K} |y_g[n]|^2}. \tag{4}$$

Note that, the conventional narrowband signal acquisition is a special case of the above signal model with $M = 1$. Figure 1 shows the block diagram for the proposed wideband signal acquisition scheme. Let the bandwidth of the spectrum holes that need to be found be denoted by W_h, such that $W_h = N_e f_b$. With this setting, the task of the sensing algorithm is to find a set of $N_e (\ll N)$ *consecutive* unoccupied bins in the given wideband. We discuss this in the next section.

III. The M-Bin Group Test Design

Using the above data acquisition scheme, we first describe an algorithm to find a contiguous spectrum hole of the specified bandwidth of N_e bins. Let the parameters N and M be as defined in the previous section. Let N_e be an integer multiple of M and define[1] $b = N_e/M$. In each test, the proposed algorithm makes an occupancy decision on a group of $M \leq N_e$ contiguous bins. Such group tests, referred to as M-bin tests, are conducted sequentially on multiple adjacent groups until b consecutive M-bin tests declare the set of bins being tested as unoccupied. Also, for simplicity, we assume that the required N_e empty bins can be found using one pass of the algorithm over the given wideband consisting of N bins. This holds true when the occupancy of the primary is sparse in the frequency domain and $N_e \ll N$, which is typically the case in scenarios relevant for CR deployment.

An M-bin group test forms the basic building block of the above algorithm to find N_e unoccupied bins. Let $\mathcal{H}_l$ denote the hypothesis that l out of M bins are occupied in the group under test and let $\{\mathcal{H}_l\}_{l=1}^{M}$ denote the composite alternate hypothesis, i.e., $\mathcal{H}_l$ is true for some $l = 1, 2, \ldots, M$. An M-bin group test distinguishes between the following hypotheses:

$$\begin{aligned} \mathcal{H}_0 &: \quad \text{No primary signal on any of the } M\text{-bins} \\ \{\mathcal{H}_l\}_{l=1}^{M} &: \quad \text{Primary signal present on at least one bin.} \end{aligned} \tag{5}$$

To find N_e empty bins, the algorithm can use different values of M (and hence b) and K. We first describe the algorithm with a fixed value of M and K, and later present a way of choosing the best M and K. The following optimization problem arises naturally in the context of the M-bin test:

$$\textit{minimize} \quad \overline{N}_t \qquad \text{subject to} \qquad P_e \leq P_0, \tag{6}$$

where P_e denotes the probability that the overall search algorithm makes an error, and $\overline{N}_t$ denotes the average number of tests required to find N_e consecutive bins. The minimization in (6) is over the parameters M, b, K and the detection thresholds used in the M-bin tests. Since the algorithm terminates once it has declared a set, say $\mathcal{A}$, of N_e consecutive bins as unoccupied, we say that an error has occurred if the primary signal is present in one or more of the bins in $\mathcal{A}$. Mathematically,

$$\begin{aligned} P_e \triangleq \Pr\,(&\text{Primary present in a set } \mathcal{A} \text{ of } N_e \text{ bins} \mid b \\ &\text{consecutive } M\text{-bin tests succeed for the first time}). \end{aligned} \tag{7}$$

Note that, P_e is related to the miss detection probability, i.e., the probability that the group $\mathcal{A}$ is declared as empty given that at least one bin in $\mathcal{A}$ is actually occupied, through Bayes' rule. Also, a false alarm event, i.e., the event that $\mathcal{A}$ is declared occupied given that it is actually empty, leads to an increased detection delay; its effect is captured in $\overline{N}_t$. See Proposition 1 and Appendix B.

Let occupancy across the bins be i.i.d. and distributed as binary Bernoulli random variables (denoted $\sim \mathcal{B}(\rho)$), where ρ is the fraction of bins occupied on average, over the long term. In the current work, we focus on the i.i.d. occupancy model [18], that, apart from being analytically tractable, might also be of independent interest in the area of adaptive group testing where the items being defective is independent of each other. We further assume that the occupancy pattern stays fixed over the search duration. Let H_{0d} denote the event that $\mathcal{H}_0$ was declared by a single group test and define $p \triangleq Pr\{H_{0d}\}$. Let Π_0 and Π_1 represent the prior probabilities for the null and alternate hypotheses for the M-bin group test. With our

[1]We consider such a combination of N_e and M for the simplicity of exposition. The algorithm can be easily adapted to non-integer multiples also.

This article has been accepted for publication in a future issue of this journal, but has not been fully edited. Content may change prior to final publication. Citation information: DOI 10.1109/TVT.2014.2305978, IEEE Transactions on Vehicular Technology

assumptions, $\Pi_0 = (1-\rho)^M$ and $\Pi_1 = 1 - \Pi_0$. Define $P_{me} \triangleq Pr\{\{\mathcal{H}_l\}_{l=1}^M | H_{0d}\}$ as the probability that the single group test makes an incorrect decision, given that the group test has declared $\mathcal{H}_0$. The following proposition connects P_e and $\overline{N}_t$ to P_{me} and p, the parameters of the M-bin group test.

Proposition 1. *Let $\overline{N}_t$, M, b, P_e, P_{me}, and p be as defined above. Then the following hold:*

$$P_e = 1 - (1 - P_{me})^b \quad \textit{and} \quad \overline{N}_t = \sum_{i=1}^{b} (p)^{-i}. \tag{8}$$

Proof: See Appendix A.

From Proposition 1, $\overline{N}_t$ depends solely on p and b, and is monotonically decreasing with p. Thus, the design goal for the single M-bin test can be stated as

$$\textit{maximize} \quad p \qquad \text{subject to} \qquad P_{me} \leq P_0', \tag{9}$$

where $P_0' = 1 - (1 - P_0)^{(1/b)}$. The maximization above is over all possible decision rules, denoted by $\delta(T)$. Our next proposition establishes that a Likelihood Ratio Test (LRT) [24] is optimal for the design criterion specified in (9). Let $\delta_L(T)$ be a decision rule based on the LRT with threshold $\eta_{gt} > 0$, defined as $\delta_L(T) = 1, Pr\{T|\{\mathcal{H}_l\}_{l=1}^M\} \geq \eta_{gt} Pr\{T|\mathcal{H}_0\}$, and $= 0$ otherwise, where T is given by (4). We state:

Proposition 2. *Let $\delta_L(T)$ be the LRT decision rule defined above, with η_{gt} chosen such that $P_{me}(\delta_L) = P_0'$. Let $\delta'(T)$ be any other decision rule such that $P_{me}(\delta') \leq P_0'$. If $\eta_{gt} > \Pi_0 P_0'/\{\Pi_1(1-P_0')\}$, then $\overline{N}_t(\delta_L) \leq \overline{N}_t(\delta')$, where $\overline{N}_t(\delta_L)$ (or $\overline{N}_t(\delta')$) represents the average number of tests required to find a consecutive set of N_e vacant bins using the test δ_L (or δ').*

Proof: See Appendix B.

To compute likelihood ratios, we need the probability distributions of the test statistic defined in (4) under the two hypotheses. To this end, we need to know the variances under the primary signal present hypothesis $\{P_l\}_{l=1}^M$, but these are unknown and in general hard to estimate. To get around the problem of unknown $\{P_l\}$, we define a bin as being occupied if the received primary signal power in the bin is at least P_s. Further, we *design* the test conservatively by assuming that the received primary signal power in any occupied bin *equals* P_s. This is in line with the approach recommended in emerging CR standards such as the IEEE 802.22, where the CR is required to reliably sense the primary signal whenever the received signal power exceeds -116dBm [25]. With these assumptions, it can be shown that

$$\begin{aligned} \mathcal{H}_0 : T &\sim \mathcal{N}\left(m_0, \sigma_0^2\right) \\ \{\mathcal{H}_l\}_{l=1}^M : T &\sim \sum_{l=1}^{M} \theta_l \mathcal{N}\left(m_l, \sigma_l^2\right), \end{aligned} \tag{10}$$

where $\sigma_l^2 \triangleq \left(M\sigma^2 + lP_s\right)/2$, $m_l \triangleq \sqrt{(2K-1)\,\sigma_l^2}$ and $\theta_l \triangleq \left[\binom{M}{l}\rho^l(1-\rho)^{M-l}\right]/\Pi_1$, such that $\sum_{l=1}^M \theta_l = 1$. In deriving the above distributions, we have used the approximation that if $X \sim \chi^2(K)$, then $\sqrt{2X} \sim \mathcal{N}\left(\sqrt{2K-1}, 1\right)$ ([26], Ch. 26).

The log-likelihood function corresponding to the test in (10) is analytically intractable, making it hard to obtain the detection threshold in closed form. However, it can be easily shown that it is approximately quadratic in T (when $M = 1$, it is exactly quadratic in T. For $M > 1$, when one of the terms in the mixture density dominates the other terms for T close to the threshold, the error in the approximation is small.) Due to this, the critical region is of the form $\left\{\{T \leq \eta_{gt0}'\} \cup \{T \geq \eta_{gt1}'\}\right\}$, where η_{gt0}' and η_{gt1}' are lower and upper thresholds. For most scenarios of interest, the contribution to P_{me} from $\{T \leq \eta_{gt0}'\}$ is small, since it represents the unlikely event that, due to its larger variance, the instantiation of the received signal power estimate under $\{\mathcal{H}_l\}_{l=1}^M$ is unusually small. This allows us to replace the LRT test by a simple, albeit sub-optimal, one-sided threshold test on T:

$$T \underset{\mathcal{H}_0}{\overset{\mathcal{H}_1}{\gtrless}} \eta_{gt1}'. \tag{11}$$

The threshold η_{gt1}' is chosen to satisfy the constraint on P_{me} in (9). For notational simplicity, let η be the threshold used in the test. Define the false alarm and miss detection rate of a single M-bin test as $\alpha(\eta) \triangleq \Pr\{\{\mathcal{H}_l\}_{l=1}^M \text{ declared}|\mathcal{H}_0\} = \Pr\{T \geq \eta|\mathcal{H}_0\}$ and $\beta(\eta) \triangleq \Pr\{\mathcal{H}_0 \text{ declared}|\{\mathcal{H}_l\}_{l=1}^M\} = \Pr\{T < \eta|\{\mathcal{H}_l\}_{l=1}^M\}$, respectively. Also, define $\beta_l \triangleq \Pr\{\mathcal{H}_0 \text{ declared}|\mathcal{H}_l\}$, i.e., the miss detection rate when exactly l bins are occupied. These can be computed as

$$\begin{aligned} \alpha(\eta) &= 1 - Q\left(\frac{m_0 - \eta}{\sigma_0}\right), \\ \beta(\eta) &= \sum_{l=1}^{M} \theta_l \beta_l \quad \text{where} \quad \beta_l = Q\left(\frac{m_l - \eta}{\sigma_l}\right), \end{aligned} \tag{12}$$

where m_l and θ_l are as defined in (10). The constraint on P_{me} in (9) leads to the following nonlinear equation, the solution to which yields η_{gt1}':

$$\frac{\beta(\eta)\,\Pi_1}{p(\eta)} = P_0', \tag{13}$$

where $p(\eta)$ can be computed as

$$p(\eta) = \Pi_0\left(1 - \alpha(\eta)\right) + \Pi_1 \beta(\eta). \tag{14}$$

Numerical techniques such as the bisection method have to be used to solve (13) to obtain η_{gt1}'.

This completes the design for an M-bin group test using given values of the number of samples, K, and the group size, M. In the next section, we show how to find an optimal value for K and M.

IV. Optimal Parameters for the M-Bin Test

We start by describing a procedure for finding the optimal K. Note that, (13) can be written as

$$\Gamma(\eta, K) = C_1, \tag{15}$$

where $C_1 = \Pi_0 P_0'/[\Pi_1(1 - P_0')] > 0$, and $\Gamma(\eta, K) \triangleq \{\sum_{l=1}^M \theta_l Q(z_l)\}/Q(z_0)$, with z_l, for $l = 0, 1, \ldots, M$, defined as

$$z_l \triangleq \frac{(m_l - \eta)}{\sigma_l} = \sqrt{2K-1} - \frac{\eta}{\sigma_l}. \tag{16}$$

This article has been accepted for publication in a future issue of this journal, but has not been fully edited. Content may change prior to final publication. Citation information: DOI 10.1109/TVT.2014.2305978, IEEE Transactions on Vehicular Technology

Since σ_l increases with l, as seen from (10), z_l also increases with l for a fixed K, i.e., $z_0 < z_1 < \cdots < z_M$. We first study the variation of Γ with η and K. Although K is an integer valued variable, for the purpose of analysis, we treat K as a positive real number. Due to the continuity of the Q-function, $\Gamma(\eta, K)$ is continuous with respect to η and K, and since $z_l > z_0$, $0 < \Gamma(\eta, K) < 1$. Further, we have:

Proposition 3. *(a) For fixed K, $\Gamma(\eta, K)$ is a quasi-convex function of η and attains a minimum value, $\Gamma_{\min}(K) = \Gamma(\eta_0, K)$, where η_0 satisfies $\frac{\partial \Gamma(\eta,K)}{\partial \eta}\Big|_{\eta=\eta_0} = 0$, i.e.,*

$$\sum_{l=1}^{M} \theta_l \left[\frac{Q(z_0)e^{-z_l^2/2}}{\sigma_l} - \frac{Q(z_l)e^{-z_0^2/2}}{\sigma_0} \right] = 0, \qquad (17)$$

where z_l, $l = 0, 1, \ldots, M$ are evaluated at η_0.

(b) For fixed η, $\Gamma(\eta, K)$ is a decreasing function of K.

Proof: See Appendix C.

Figure 2 depicts the behavior of $\Gamma(\eta, K)$ as implied by the above proposition. We make the following remarks: *(a) For a given probability of incorrect detection, P_0', there is a certain minimum number of samples, $K_{\min}(\geq 1)$, that are required to set up the M-bin group test to satisfy the performance requirement P_0'.* In fact, if $K_0(\geq 1)$ is such that $\Gamma_{\min}(K_0) > C_1$ (e.g., with $K = 20$ in Figure 2), a test cannot be designed with K_0 samples. However, since $\Gamma_{\min}(K)$ is a decreasing function of K, we can find the smallest integer, denoted $K_{\min}$, such that $\Gamma_{\min}(K_{\min}) \leq C_1$. For any $K \geq K_{\min}$, an M-bin test can be designed and each will result in a different average number of tests required to find N_e unoccupied bins. *(b)* For each $K \geq K_{\min}$, due to the quasi-convex nature of $\Gamma(\eta, K)$, there exist exactly two solutions of (15), and since the M-bin test is a threshold test, we pick the larger of the two as the threshold to be used. Define $\eta_s(K)$, the computed threshold for a given value of K, as

$$\eta_s(K) = \max \{\eta \ : \ \Gamma(\eta, K) = C_1\}. \qquad (18)$$

Note that, due to the way η_s is chosen, $\frac{\partial \Gamma(\eta,K)}{\partial \eta}\Big|_{\eta=\eta_s} > 0$. Also, since $\Gamma(\eta, K)$ decreases with K, it is easy to see that $\eta_s(K)$ is an increasing function of K.

For each $K \geq K_{\min}$, a test that satisfies the constraint on the probability of incorrect decision can be designed; and our next task is to decide which K to use. Note that, since $M \leq N_e$, multiple M-bin tests are required to find N_e consecutive unoccupied bins. To run the test on a different set of M bins, we need to move to a different center frequency. Due to the time required by various Radio Frequency (RF) components such as the phase-locked loop, oscillators, etc, to reach a steady state after the change in center frequency, there is a setup delay (also referred to as the settling time) of N_S samples associated with each M-bin test [15]. Thus, we define the following objective function:

$$D_{\text{avg}}(K) = \overline{N}_t(K)\,(K + N_S). \qquad (19)$$

$D_{\text{avg}}(K)$ can be viewed as the average search duration for finding N_e unoccupied bins with an M-bin test designed with K samples. The value of N_S is known, as it depends on the front-end RF chain at the CR, and is part of its technical specifications. From (19), N_S plays significant role in the time taken to find N_e bins when it is comparable to K or when $\overline{N}_t(K)$ is high. We state the following:

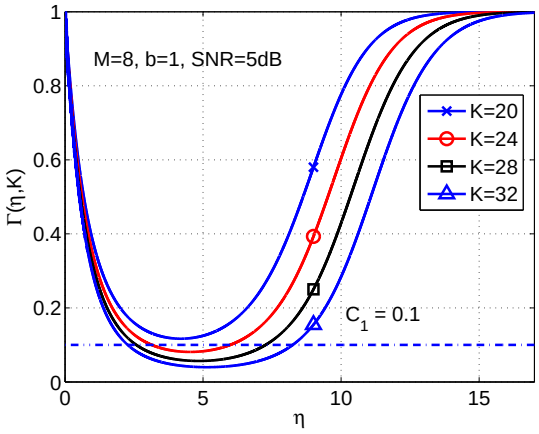

Fig. 2. Family of $\Gamma(\eta, K)$ functions: increasing K helps in meeting the minimum performance target.

Proposition 4. *For $K \geq K_{\min}$, $D_{avg}(K)$ is a convex function of K.*

Proof: See Appendix D.

Thus, for a given M, the optimum K can be computed as the solution to:

$$K_{\text{opt}} = \underset{K \geq K_{\min}}{\textit{minimize}} \quad D_{\text{avg}}(K). \qquad (20)$$

With regards to minimization, $D_{\text{avg}}(K)$ is a well-behaved function and simple convex optimization techniques, e.g., the Newton method [27], can be used to find the optimum K. Note that the computational complexity of evaluating K_{opt} (and η_{gt}' in (13)) is not of major concern here, as these will be computed offline and remain unchanged as long as the primary usage statistics remain the same. In the above analysis, we have assumed K to be a real number. In practice, we compute $D_{\text{avg}}(K)$ at the two integers nearest to the optimum real value and pick K_{opt} to be the one with smaller $D_{\text{avg}}(K)$. Figure 3 illustrates the convex behavior of $D_{\text{avg}}(K)$ with K for a particular set of operating parameters.

The last step in the design of the detector is to find the optimum combination (M, b) that minimizes the average detection delay. To this end, for a given M, let $K_{\text{opt}}(M)$ be the number of samples that minimize the average search duration to find $N_e = Mb$ consecutive unoccupied bins. We use $D_{\text{avg}}(K_{\text{opt}}(M))$ as the metric to compare the performance with different values of M. Let $\mathcal{M} = \{(M, b) : b = \lceil N_e/M \rceil\}$ be the set of all combinations of (M, b) that can be used to find N_e consecutive empty bins. To find the optimal value of M for a given test scenario, we minimize $D_{\text{avg}}(K_{\text{opt}})$ over $\mathcal{M}$:

$$(M_{\text{opt}}, b_{\text{opt}}) = \underset{(M,b)\in\mathcal{M}}{\textit{minimize}} \quad D_{\text{avg}}\left(K_{\text{opt}}\left(M\right)\right). \qquad (21)$$

We solve the above optimization problem by simply searching over the set $\mathcal{M}$, since there are only a finite number of

This article has been accepted for publication in a future issue of this journal, but has not been fully edited. Content may change prior to final publication. Citation information: DOI 10.1109/TVT.2014.2305978, IEEE Transactions on Vehicular Technology

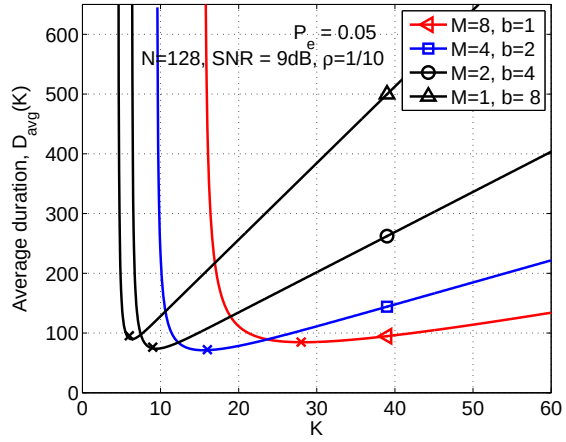

Fig. 3. $D_{\text{avg}}(K)$ is convex in K: Minimizing $D_{\text{avg}}(K)$ leads to an optimal value of K; '$\times$' markers show the experimental $D_{\text{avg}}(K)$ at computed K_{opt}.

combinations, and computing $D_{\text{avg}}\left(K_{\text{opt}}\left(M\right)\right)$ is not computationally demanding. Thus, given the operating parameters: (σ^2, ρ, P_s), we have fully specified an M-bin test, and a method to choose the (M, K) that minimizes the average delay in searching for a spectrum hole consisting of N_e consecutive unoccupied bins.

V. Multi-Stage Sensing Algorithm

In this section, we describe an M-bin test based multi-stage sensing algorithm, to find the available spectrum holes in a given wideband of interest. The basic idea, as shown in Figure 4, is to search for spectrum holes of different bandwidths by making multiple passes of search on a given wideband. With each successive pass, the width of the hole (specified by the value of M used in the M-bin test) being searched for is halved, and only the parts of the wideband that have been declared occupied in the previous stages are considered in the search. A multi-stage algorithm can be used, for example, in spectrum hole search with a frequency hopping primary. Here, the occupancy pattern keeps changing periodically, and we refer to this time interval as hopping interval, denoted by N_h.[2] In terms of CR usage, each hopping interval is split into two phases: a *sensing phase*, to find the unoccupied spectrum, and a *usage phase*, to exploit the spectrum hole found. Let n represent the time duration of the sensing phase. Thus, the goal for sensing algorithms in a frequency hopping scenario is to maximize $N_{TB} \triangleq M_h(n)(N_h - n)$, where $M_h(n)$ is the number of unoccupied bins found during the sensing phase. In other words, we want as much usable spectrum for as much time as possible in a given hopping interval.

Let M, ρ, K_{opt}, η_s and p be as defined earlier. Let $M^{(l)}$, $\rho^{(l)}$, $K_o^{(l)}$, $\eta_s^{(l)}$ and $p^{(l)}$ denote the values of above parameters at the l^{th} stage. Let L be the number of stages. Since, at each stage, the value of M is halved, $M^{(1)} = 2^{L-1}$. Let P_{ems} denote the bin-level error probability in the sense of (7), i.e., the probability that an individual bin is actually occupied given that it has been declared unoccupied by the algorithm. An overall bin-level error probability constraint can be satisfied if the M-bin test at every stage satisfies the same bin-level error probability constraint. For an M-bin test, define $P_{me}^{(i)} \triangleq$ Pr (i^{th} bin in $\mathcal{A}_M$ is occupied $\mid$ $\mathcal{A}_M$ is declared unoccupied), where $\mathcal{A}_M$ is the set of M bins being tested. That is, $P_{me}^{(i)}$ quantifies the bin-level error probability of an M-bin test. It can be shown that $P_{me}^{(i)} = P_0$, i.e., it meets the target error probability constraint, if the threshold used in the M-bin test, η, is chosen as the solution to the following equation:

$$\sum_{k=1}^{M} \binom{M-1}{k-1} \rho^k (1-\rho)^{M-k} \frac{\beta_k(\eta)}{p(\eta)} = P_0. \qquad (22)$$

Here, ρ denotes the occupancy rate, $\beta_k(\eta)$ and $p(\eta)$ are as defined in (12) and (14), respectively. Thus, depending upon P_0, M and ρ, an M-bin test satisfying a specified bin-level error probability constraint can be designed by choosing the detection threshold according to the above equation. We also note that since each stage removes a part of the unoccupied spectrum from the given band of operation, the occupancy rate, $\rho^{(l)}$, for each stage needs to be updated accordingly.

We now describe the multi-stage algorithm. Let an estimate of the number of bins found at the end of the l^{th} stage be denoted by $T_f(l)$.[3] Let ρ_0 be the occupancy rate for the wideband over which multi-stage algorithm is operating. Let $P_0 \in (0\ 1)$ denote the target bin-level error probability.

1) Initialize: $\rho^{(1)} = \rho_0$; $T_f(0) = 0$; and set all the bins in the wideband as occupied.
2) For $l = 1, 2, \ldots, L$
   a) Using $M = M^{(l)}$, $\rho = \rho^{(l)}$ and P_0, find the detection threshold, $\eta_s^{(l)}$, using (22).
   b) Find the optimum number of samples, $K_o^{(l)}$, using (20) with $b = 1$. That is, find the number of samples required to minimize the detection delay in finding a spectrum hole of size M. Also, find the corresponding $p^{(l)}$ using (14).
   c) Make a pass over the full wideband, i.e., perform a series of M-bin tests for the bins that are set as occupied, with $M = M^{(l)}$, $K = K_o^{(l)}$ and $\eta = \eta_s^{(l)}$. If a test declares $\mathcal{H}_0$, then set the corresponding $M^{(l)}$ bins as unoccupied.
   d) Update $T_f(l)$: $T_f(l) = T_f(l-1) + [N - T_f(l-1)]\, p^{(l)}$.
   e) Update the occupancy rate for the next stage: $\rho^{(l+1)} = \{N\rho - T_f(l)P_0\}/\{N - T_f(l)\}$.
   f) Update $M^{(l+1)} = M^{(l)}/2$.

Note that, the above algorithm ensures that the overall bin-level error probability constraint is met, since each stage is designed such that the bin-level error probability in that stage is P_0. Also, the above update for the occupancy rate works well when the primary powers in the different bins are approximately equal and known. In the unequal or unknown transmit power case, the M-bin test ensures that the empirical

[2] For example, in a Bluetooth network, the hopping time is $1/1600$ s. With a sampling rate of 2 MHz, this implies $N_h = 1250$.

[3] Note that, this can also be replaced by the number of bins that are declared as unoccupied in the actual running of the algorithm. Here, we use an estimate of the number of bins declared as unoccupied in order to facilitate an offline calculation of the thresholds to be used at each stage, and to analytically compute the detection delay.

This article has been accepted for publication in a future issue of this journal, but has not been fully edited. Content may change prior to final publication. Citation information: DOI 10.1109/TVT.2014.2305978, IEEE Transactions on Vehicular Technology

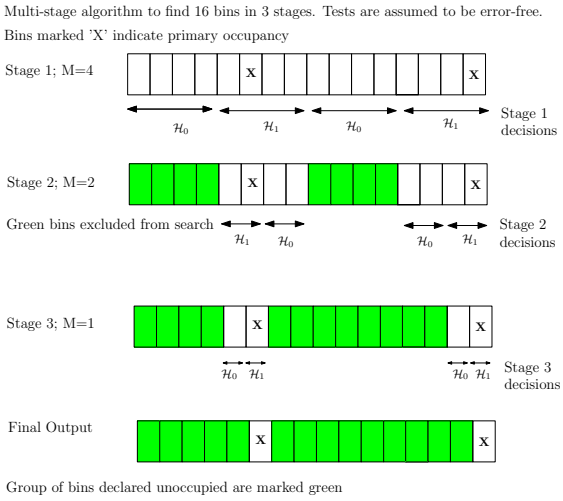

Fig. 4. A pictorial illustration of the multi-stage algorithm.

values of $P_{me}^{(i)}$ remain below the specified target. We have observed, via simulations, that the algorithm works well in terms of the detection delay, and also satisfies the specified target error rates. When $M^{(1)} = 1$, we get the conventional bin-by-bin detection scheme as a special case, as before.

VI. Simulations and Results

We now present simulation results to illustrate the performance of the proposed signal acquisition scheme and spectrum hole search algorithms. We first present the results for the contiguous hole search algorithm in the AWGN case. We consider a test setup with $N = 128$, $N_e = 8$ and $\rho \in \{1/6, 1/8, 1/10, 1/12, 1/16, 1/20\}$. The signal samples used for computing the test statistic are generated according to (3). The signal powers for bins with occupancy, P_l, are chosen uniformly at random from the set $\{P_s, P_s+2, P_s+4, P_s+6\}$ dB, with $P_s = 0$ dB. We refer to P_s/σ^2 as the detection SNR, and vary it from 0 to 13 dB. The test outputs a sequence of N_e bins that are declared unoccupied. An error occurs if this declared set contains any occupied bin. The target error rate constraint is set as $P_0 = 0.1$. For different combinations of (M, b), the value of K_{opt} is numerically computed, and the corresponding detection delay ($D_{\text{avg}}(K_{\text{opt}})$, henceforth denoted D_{avg} for short) performance is evaluated. For calculating D_{avg}, we used $N_S = 0$.

Figures 5 and 6 show the variation of D_{avg} with sparsity and SNR, respectively. As expected, with increasing sparsity, the group tests with higher M perform better. At low SNR, $M = 1$ is optimal. As the SNR increases, $M > 1$ outperforms $M = 1$, and interestingly, the relative reduction in D_{avg} is higher for higher M. Note that, the bin-by-bin ($M = 1$) test can be considered to be the result of using the framework in [19] when the primary transmitter to secondary receiver channel gain information is absent and the test is designed to minimize the average test duration. We evaluate the performance of the group tests with the optimal values of M, K and η_s computed as described in Section III. We see that the tests with optimal parameter values perform the best in all the simulated scenarios. In Figure 7, we show the excellent match between the simulation and analytical results for D_{avg} and P_e at different sparsity values, when $P_l = P_s$. We have also empirically verified that the observed P_e is below the target $P_0 = 0.1$. Further, we have found that the collective impact of all of the approximations used in the above development on the detection delay performance and the probability of incorrect decision is negligible, as argued in the preceding sections. However, we omit the detailed results here for the sake of brevity.

Next, we consider the scenario where the primary signals undergo Rayleigh multi-path fading and lognormal shadowing with variance 4 dB. Figure 8 shows the variation of D_{avg} with detection SNR. We see the same behavior as in the AWGN case, albeit at roughly 7dB higher SNR values. This is expected, as the M-bin detector is an energy based detector and its performance degrades in the presence of fading.

Table I shows the reduction in D_{avg} compared to tests with $M = 1$ at an SNR of 9 dB for the AWGN case and 16 dB for the fading case, and with different sparsity values. With $N_S = 0$, the reduction in D_{avg} of the proposed group test compared to the $M = 1$ case is 20 to 30%, depending on the sparsity level. For a conservative value[4] of $N_S = 5$, the percentage reduction in D_{avg} is significantly higher, and varies between 35 and 60%. This is because tests with higher M result in a significantly lower average number of tests (see Table II) and thus save on the test setup overheads, compared to the $M = 1$ case.

Figure 9 shows the variation of $D_{\text{avg}}(M_{\text{opt}}, K_{\text{opt}})$ with primary SNR for different values of target P_0 in the AWGN case. It is interesting to note that the curves are approximately linear, even though different values of M are optimal for different primary SNRs. Also, larger sensing times are required to satisfy smaller values of the target probability of error, as expected.

We now compare the performance of the M-bin detector with the energy-based Single Slot Detector (SSD) proposed in [28]. We use the same setup as in [28], and study the achievable opportunistic secondary throughput, $R(\tau)$, defined as, $R(\tau) \triangleq C_0(1 - \tau/T_F)(1 - P_f)(1 - \rho)B$ bits/s, where τ is the sensing (search) duration, T_F is the frame duration and C_0 is the secondary throughput when the primary is absent, ρ is the prior probability of the primary being present and B is bandwidth of a single slot. We assume that the secondary network does not obtain any throughput if it transmits data in the presence of the primary (that is, C_1, as defined in [28], is zero). Note that, P_f is the probability of false alarm obtained by designing the detector to ensure that the probability of miss stays below a specified target. The M-bin detector searches M consecutive adjacent slots simultaneously in each test, and the corresponding secondary throughput is given by: $R(\tau) \triangleq MC_0(1 - \tau/T_F)(1 - P_{fM})(1 - \rho)^M B$ bits/s, where P_{fM} is the probability of false alarm for an M-bin detector with the given target probability of miss detection. We assume BPSK signaling, a sampling rate of 6 MHz, $C_0 = 6.6582$ (which corresponds to a secondary-to-secondary SNR of 20 dB), and

[4]At a sampling rate of 1 MHz and with a low-power phase-locked loop (see [15], Table I), N_S can be as high as 120 samples.

This article has been accepted for publication in a future issue of this journal, but has not been fully edited. Content may change prior to final publication. Citation information: DOI 10.1109/TVT.2014.2305978, IEEE Transactions on Vehicular Technology

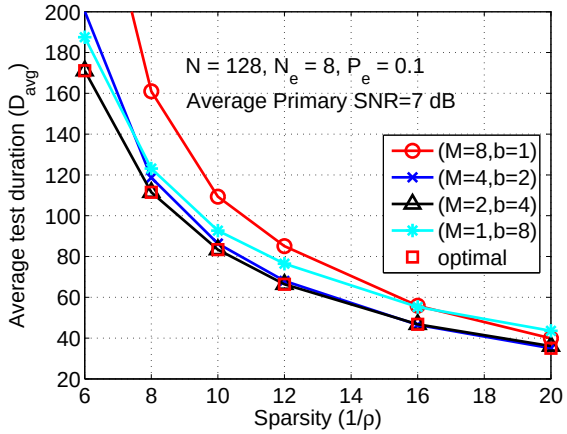

Fig. 5. D_{avg} *Vs.* Sparsity in the AWGN case. At higher sparsity, group tests outperform the bin-by-bin test.

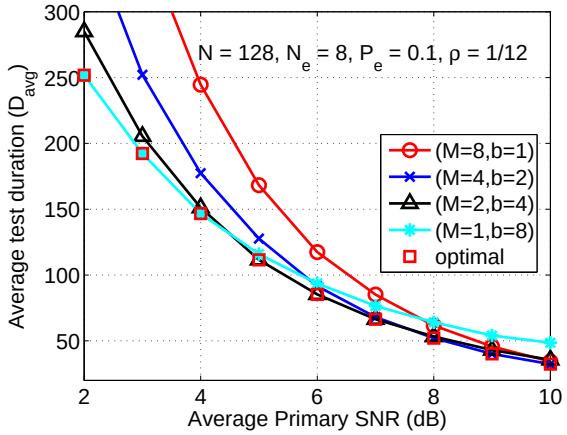

Fig. 6. D_{avg} *Vs.* SNR in the AWGN case. At higher SNRs, group tests outperform the bin-by-bin test.

TABLE II
AVERAGE NUMBER OF TESTS FOR VARYING SPARSITY AT SNR = 9DB.

Sparsity	1/6	1/8	1/12	1/16
$M = 8,\ b = 1$	5.6	3.8	2.6	2.1
$M = 4,\ b = 2$	7.9	5.9	4.4	3.9
$M = 2,\ b = 4$	12.6	9.0	7.1	6.2
$M = 1,\ b = 8$	21.8	17.5	13.5	12.8

a target probability of miss of 0.1, as in [28]. Figure 10 compares the normalized throughputs $R(\tau)/B$ for different values of τ for the scenario where $\rho = 0.1$, $T_F = 100$ ms and a primary SNR value of -13 dB. Also, Table III compares the achievable throughput for different operating scenarios. As the SNR and sparsity increase, M-bin tests with larger M provide the best secondary throughput, and the group test significantly outperforms the SSD.

We now present a few representative results that illustrate the key aspects of multi-stage algorithm discussed in Section V. Here, we consider the AWGN case and an i.i.d. occupancy model with $N = 256$. We first investigate the application of the multi-stage algorithm for finding non-contiguous spectrum holes in the case with equal power primary signals. Figure 11 shows the results of running the multi-stage algorithm with different values of $M^{(1)}$, i.e., with different number of stages. It can be observed that, depending upon the number of non-contiguous unoccupied bins we wish to find, different multi-stage instantiations lead to faster search times. For example, $M^{(1)} = 8$ (i.e., $L = 4$) is optimal if we wish to find about 100 unoccupied bins, whereas $M^{(1)} = 4$ (i.e., $L = 3$) is optimal if we wish to find about 200 unoccupied bins. Figure 12 shows the results for the spectrum hole search in the presence of frequency hopping. For the multi-stage algorithm with different initial group sizes and different search durations, we need to pick the one that maximizes N_{TB}, as defined in Section V. It can be seen that, under sparse spectrum occupancy by the primary, the group testing based sensing schemes are more efficient in harvesting the available spectrum in a given hopping interval. For example, at an SNR$=$ 7dB, multi-stage instantiations with $M^{(1)} = 2,\ 4$ and 8 all have higher maximum N_{TB} compared to the bin-by-bin test.

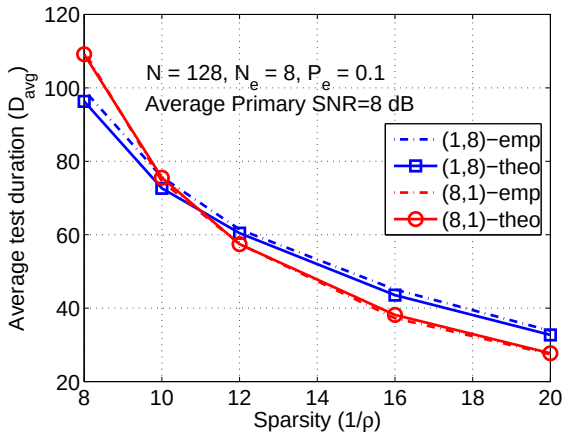

Fig. 7. Good match with theoretical results, D_{avg} *Vs.* Sparsity in the AWGN case. Empirical P_e for the above data points: Case ($M = 8, b = 1$): $[0.092\ 0.093\ 0.095\ 0.095\ 0.097]$ and Case ($M = 1, b = 8$): $[0.084\ 0.090\ 0.091\ 0.100\ 0.094]$ at sparsity values of $1/\rho = [8\ 10\ 12\ 16\ 20]$, respectively. The empirical P_e always remains below the target value of 0.1.

VII. CONCLUSIONS

In this work, we investigated the use of adaptive group testing based techniques for spectrum hole search in cognitive radios. To enable this, we proposed a signal acquisition scheme that deliberately introduces aliasing by sampling a wideband signal at a sub-Nyquist rate. We developed spectrum hole search algorithms based on the energy of the aliased signal. The algorithms exploit the sparsity in the primary spectral occupancy by making a joint occupancy decision on the group of narrowband bins over which the signal is acquired. We first designed the group testing based algorithm to search contiguous spectrum holes while guaranteeing a given level of protection to the primary network. We extended the group tests to a multi-stage sensing algorithm that looks for contiguous holes of different widths at each stage. Based on the theoretical analysis of the group tests, we provided a computational procedure to obtain the optimal group size, number of samples, and the detection thresholds, that minimize the average search

This article has been accepted for publication in a future issue of this journal, but has not been fully edited. Content may change prior to final publication. Citation information: DOI 10.1109/TVT.2014.2305978, IEEE Transactions on Vehicular Technology

TABLE I
PERCENTAGE D_{AVG} REDUCTION COMPARED TO $M = 1$.

Sparsity	1/8		1/12		1/16	
	$N_S = 0$	$N_S = 5$	$N_S = 0$	$N_S = 5$	$N_S = 0$	$N_S = 5$
(Reduction, M): AWGN, 9dB	(19%, 4)	(43%, 4)	(26%, 4)	(52%, 8)	(29%, 4)	(61%, 8)
(Reduction, M): Fading, 16dB	(21%, 4)	(44%, 4)	(26%, 4)	(52%, 8)	(30%, 4)	(62%, 8)

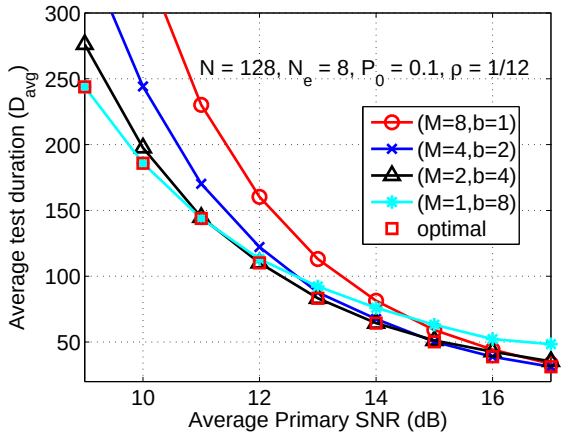

Fig. 8. Contiguous hole search, with fading and shadowing, D_{avg} *Vs.* SNR: Similar trends as compared to AWGN case, but at higher SNRs.

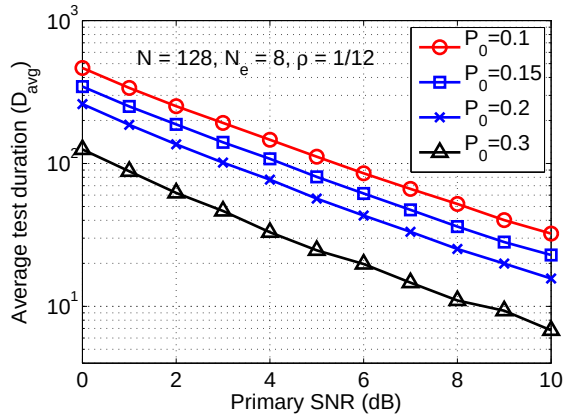

Fig. 9. Contiguous hole search, AWGN, D_{avg} *Vs.* SNR: Performance at different target error probabilities.

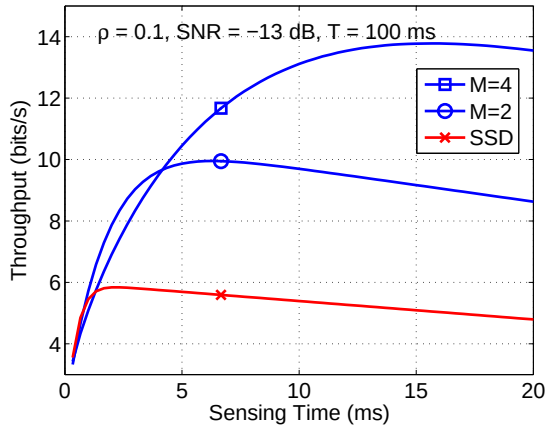

Fig. 10. Normalized throughput vs. the sensing time: M-bin detector significantly improves secondary throughput. "SSD" refers to the energy-based single slot detection scheme in [28].

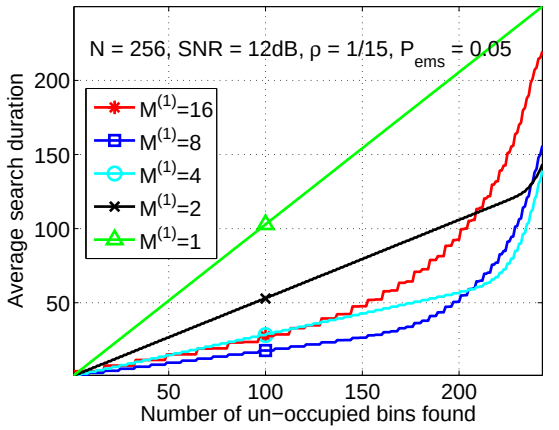

Fig. 11. Search durations for different multi-stage instantiations.

duration given a target error rate constraint. This enabled us to identify the operating parameter regimes where group testing based algorithms outperform their narrowband counterparts. The performance gains are achieved at a minimal additional hardware cost, which makes the group testing based sensing schemes attractive for practical implementation.

APPENDIX

A. Proof of Proposition 1

From the definition of P_e in (7), it follows that the algorithm makes an error if any of the last b M-bins tests, that have all declared $\mathcal{H}_0$, make an error. Thus,

$$P_e = 1 - \Pr\,(\text{None of the last } b \text{ } M\text{-bin tests is in error} \mid \text{All the last } b \text{ tests have declared } \mathcal{H}_0\,)$$
$$= 1 - \left(1 - \Pr(\{\mathcal{H}_l\}_{l=1}^{M} | H_{0d})\right)^b = 1 - (1 - P_{me})^b \quad (23)$$

Now, let $\overline{N}_t$ and p be as defined before. $\overline{N}_t$ can be found by setting up a recursive equation using the following arguments: (i) If we get alternate hypothesis declaration on the k^{th} attempt with $k = 1, 2, \ldots, b$, then the search process restarts since each test is independent. (ii) If we get b successive null hypothesis outputs then our search terminates. Note that declaring the alternate hypothesis on the k^{th} attempt leads to an increase in the number of tests by k. The probability that we get the first

This article has been accepted for publication in a future issue of this journal, but has not been fully edited. Content may change prior to final publication. Citation information: DOI 10.1109/TVT.2014.2305978, IEEE Transactions on Vehicular Technology

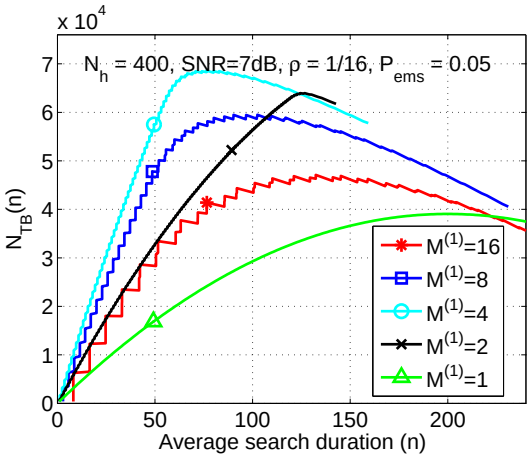

Fig. 12. Spectrum hole search and frequency hopping. Group testing based sensing exploits the available spectrum more efficiently, compared to the bin-by-bin case.

TABLE III
ACHIEVABLE THROUGHPUT, R/B BITS/S: COMPARISON OF THE M-BIN TEST WITH THE DETECTOR IN [28].

(SNR, ρ)	(-15 dB, $1/10$)	(-12 dB, $1/10$)	(-10 dB, $1/16$)
SSD	5.66	5.88	6.19
M-bin	9.09 ($M=2$)	14.81 ($M=4$)	25.13 ($M=8$)

alternate hypothesis on the k^{th} attempt is given by $p^{(k-1)}(1-p)$. Thus,

$$\begin{aligned}\overline{N}_t &= (1-p)\sum_{k=1}^{b} p^{k-1}(\overline{N}_t + k) + bp^b \\ &= (1-p^b)\overline{N}_t + (1-p)\sum_{k=1}^{b} kp^{k-1} + bp^b.\end{aligned}$$

Using

$$\sum_{k=1}^{b} kp^{k-1} = \left[\frac{1-p^{b+1}}{(1-p)^2} - \frac{(b+1)p^b}{1-p}\right],$$

and simplifying, the result follows. ■

B. Proof of Proposition 2

Let t be the random variable describing the test statistic defined in (4). Let $\mathcal{G}$ be the observation set. Let $f_0(t)$ and $f_1(t)$ denote probability distributions of t under the null and alternate hypothesis, respectively, and these are as defined in (10). Let $\alpha(\delta)$ and $\beta(\delta)$ represent the false alarm and miss detection rate, respectively, for a decision rule δ. Thus, $\alpha(\delta) = \int_{\mathcal{G}}(1-\delta(t))f_0(t)dt$ and $\beta(\delta) = \int_{\mathcal{G}}(1-\delta(t))f_1(t)dt$. From Bayes' rule, $P_{me}(\delta) = [\beta(\delta)\Pi_1]/p(\delta)$. Since $P_{me}(\delta') \leq P_0'$, (14) imply that

$$\beta(\delta') \leq \frac{P_0'}{\Pi_1}p(\delta') \quad \text{and} \quad 1-\alpha(\delta') \geq \frac{1-P_0'}{\Pi_0}p(\delta'), \qquad (24)$$

where Π_0 and Π_1 represent the prior probabilities for the null and alternate hypotheses for the M-bin group test. From the definition of $\delta_L(t)$, we have $[(1-\delta(t)) - (1-\delta(t)')][f_1(t) - \eta_{gt}f_0(t)] \leq 0$ for any $t \in \mathcal{G}$. Integrating over the entire observation space, we get

$$\beta(\delta) - \beta(\delta') \leq \eta_{gt}\left[(1-\alpha(\delta))\,(1-\alpha(\delta'))\right].$$

Using (14) and (24), we can further simplify the above to $[(1-P_0')\eta_{gt}/\Pi_0 - P_0'/\Pi_1]\,[p(\delta) - p(\delta')] \geq 0$. For $\eta_{gt} > \Pi_0 P_0'/\{\Pi_1(1-P_0')\}$, $p(\delta) \geq p(\delta')$, and the assertion follows by noting that $\overline{N}_t$ is monotonic in p. ■

C. Proof of Proposition 3

1) Part (a): For a fixed K, $z_l = \sqrt{2K-1} - \eta/\sigma_l$, $l = 0, 1, \ldots, M$ are functions of η. Hence, $\Gamma(\eta, K)$ is a real valued, continuously differentiable function of η, denoted $\Gamma(\eta)$ for short, with $\eta > 0$. Let $\Gamma'(\eta) \triangleq d(\Gamma(\eta))/d\eta$ and $\Gamma''(\eta) \triangleq d^2(\Gamma(\eta))/d\eta^2$. We use the second order conditions to prove quasi-convexity ([27], Section 3.4.3): $\Gamma(\eta)$ is quasi-convex in η, if, for all η_0 such that $\Gamma'(\eta_0) = 0$, we have $\Gamma''(\eta_0) > 0$. Since $d(Q(x))/dx = -(1/\sqrt{2\pi})e^{-x^2/2}$, and $d(z_l)/d\eta = -1/\sigma_l$ for $l = 0, 1, \ldots, M$, we have

$$\Gamma'(\eta) = \frac{1}{\sqrt{2\pi}Q^2(z_0)}\left[Q(z_0)\left[\sum_{l=1}^{M}\frac{\theta_l}{\sigma_l}e^{-z_l^2/2}\right] - \frac{e^{-z_0^2/2}}{\sigma_0}\left[\sum_{l=1}^{M}\theta_l Q(z_l)\right]\right]. \qquad (25)$$

Setting $\Gamma'(\eta) = 0$, (17) follows. We now evaluate $\Gamma''(\eta)$ at $\eta = \eta_0$ such that η_0 satisfies (17). Differentiating (25) and substituting (17), we get

$$\Gamma''(\eta_0) = \frac{1}{\sqrt{2\pi}Q(z_0)}\left[\sum_{l=1}^{M}\frac{\theta_l}{\sigma_l}e^{-z_l^2/2}\left[\frac{z_l}{\sigma_l} - \frac{z_0}{\sigma_0}\right]\right]. \qquad (26)$$

Note that z_l and z_0 are evaluated at η_0 in the above equation. Moreover, $z_0 < z_1 < \ldots < z_M$. We consider following two scenarios:

(i) $z_0 > 0$: This implies that $z_l > 0$ for all $l = 1, \ldots, M$. It is easy to show that $g(z) \triangleq zQ(z)e^{z^2/2}$ is an increasing function of $z > 0$. For any $l = 1, \ldots, M$, since $z_0 < z_l$, we get $g(z_0) < g(z_l)$, i.e., $z_0Q(z_0)e^{-z_l^2/2} < z_lQ(z_l)e^{-z_0^2/2}$. Also, $(z_0/z_l)Q(z_0)e^{-z_l^2/2} < Q(z_l)e^{-z_0^2/2}$, since $z_l > 0$. It follows that

$$\sum_{l=1}^{M}\theta_l Q(z_l)e^{-z_0^2/2} > Q(z_0)\sum_{l=1}^{M}\theta_l\frac{z_0}{z_l}e^{-z_l^2/2}. \qquad (27)$$

Using (17) and re-arranging, we get

$$\sum_{l=1}^{M}\frac{\theta_l e^{-z_l^2/2}}{\sigma_l}\frac{1}{(z_l/\sigma_l)}\left[\frac{z_l}{\sigma_l} - \frac{z_0}{\sigma_0}\right] > 0. \qquad (28)$$

Define

$$h_l \triangleq \frac{\theta_l e^{-z_l^2/2}}{\sigma_l}\frac{1}{(z_0/\sigma_0)}\left[\frac{z_l}{\sigma_l} - \frac{z_0}{\sigma_0}\right] \quad \text{and}$$

$$g_l \triangleq \frac{\theta_l e^{-z_l^2/2}}{\sigma_l}\frac{1}{(z_l/\sigma_l)}\left[\frac{z_l}{\sigma_l} - \frac{z_0}{\sigma_0}\right].$$

This article has been accepted for publication in a future issue of this journal, but has not been fully edited. Content may change prior to final publication. Citation information: DOI 10.1109/TVT.2014.2305978, IEEE Transactions on Vehicular Technology

We claim that, $\sum_{l=1}^{M} h_l > \sum_{l=1}^{M} g_l$, and from (26) and (28), it follows that $\Gamma''(\eta) > 0$. To prove the above claim let us consider the following two scenarios: (a) $g_l \geq 0$: In this case, $(z_l/\sigma_l) \geq (z_0/\sigma_0)$ and thus $h_l \geq g_l$. Hence, replacing g_l by h_l makes (28) more positive. (b) $g_l < 0$: In this case, $(z_l/\sigma_l) < (z_0/\sigma_0)$ and h_l becomes less negative compared to g_l. Hence, replacing g_l by h_l still makes (28) more positive.

(ii) $z_0 \leq 0$: For this case, we prove that $z_l/\sigma_l - z_0/\sigma_0 > 0$ for each $l = 1, \ldots, M$. From (26) it follows that $\Gamma''(\eta) > 0$. Let l_0 $(1 \leq l_0 \leq M)$ be such that $z_l < 0$ for $l \leq l_0$ and $z_l \geq 0$ for $l > l_0$. For $l > l_0$, it is straightforward to see that $z_l/\sigma_l - z_0/\sigma_0 > 0$. For $l \leq l_0$, since $z_0 < z_l < 0$, it implies $|z_l| < |z_0|$. This implies $|z_l|/\sigma_l < |z_0|/\sigma_0$ since $\sigma_l > \sigma_0$. Hence, $-|z_l|/\sigma_l > -|z_0|/\sigma_0$, thereby implying $z_l/\sigma_l - z_0/\sigma_0 > 0$, since $z_0 < z_l < 0$.

2) Part (b): For a fixed η, $\{z_0, z_1, \Gamma\}$ are functions of K. Let $\Gamma_l(K) \triangleq Q(z_l)/Q(z_0)$, and hence, $\Gamma(K) = \sum_{l=1}^{M} \theta_l \Gamma_l(K)$. We prove that each Γ_l is a decreasing function of K, and thereby prove that Γ is a decreasing function of K. Let $\Gamma_l'(K) \triangleq \partial\Gamma_l(K)/\partial K$. Using the derivative of Q-function and $dz_0/dK = dz_l/dK = 1/\sqrt{2K-1}$, we have

$$\Gamma_l'(K) = \frac{\left[Q(z_l)e^{-z_0^2/2} - Q(z_0)e^{-z_l^2/2}\right]}{\sqrt{2\pi}\sqrt{2K-1}Q^2(z_0)}. \quad (29)$$

Proving $\Gamma_l'(K) < 0$ is equivalent to proving $Q(z_l)e^{-z_0^2/2} < Q(z_0)e^{-z_l^2/2}$. We first consider the case:
$z_l > 0$ and $z_0 \geq 0$: We prove that for $z \geq 0$, $g(z) \triangleq Q(z)e^{z^2/2}$ is a decreasing function of z. Note that $g'(z) \triangleq d(g(z))/dz = e^{z^2/2}Q(z)z - 1/\sqrt{2\pi}$. We use the following upper bound for Q-function [29],

$$Q(y) < \frac{1}{(1-a)y + a\sqrt{y^2+b}} \frac{e^{-y^2/2}}{\sqrt{2\pi}},$$

for $y > 0$, $a = 0.344$ and $b = 5.334$, in the above expression, to get

$$g'(z) < \frac{1}{(1-a)z + a\sqrt{z^2+b}} \frac{1}{\sqrt{2\pi}}[az - a\sqrt{z^2+b}] < 0,$$

since, $a > 0$ and $b > 0$. And since $z_l > z_0$, this implies $Q(z_l)e^{-z_0^2/2} < Q(z_0)e^{-z_l^2/2}$. The above can be easily shown for the other cases, i.e., $\{z_l \leq 0$ and $z_0 < 0\}$, $\{z_l > 0$ and $z_0 < 0\}$, and $\{z_l > 0$ and $z_0 < 0\}$, using similar arguments.

D. Proof of Proposition 4

Define $Z_0(K) \triangleq z_0\left(\eta_s(K), K\right) = \sqrt{2K-1} - \eta_s(K)/\sigma_0$ and $Z_1(K) \triangleq z_1\left(\eta_s(K), K\right) = \sqrt{2K-1} - \eta_s(K)/\sigma_1$. From (8), we see that $N_t(K)$ depends only on $p(\eta_s(K))$ and using (14), we get $p\left(\eta_s(K)\right) = C_2 Q\left(Z_0(K)\right)$, where $C_2 = \Pi_0/(1-P_0')$. Note that $D_{\text{avg}}(K)$ is a continuous function of K (for real K). We first prove that for all $K \geq K_{\min}$, $K/Q(Z_0(K))$ is a convex function of K. Let $\Gamma(\eta, K)$, C_1 be as defined before. Let $F(K) \triangleq K/Q(Z_0(K))$, and let $z_0 \triangleq \sqrt{(2K-1)} - \eta/\sigma_0$. For a given K, $\eta(K)$ is chosen as the threshold value that satisfies $\Gamma(\eta, K) = C_1$, as given in (18). Using the quasi-convexity properties of $\Gamma(\eta, K)$ we can write $\eta(K)$ as:

$$\eta(K) = \inf_{\{\eta:\ \Gamma(\eta,K) \geq C_1\}} \eta. \quad (30)$$

For a fixed K, $Q(z_0)$ is a monotonically increasing function of η. Combining this with (30), we get

$$Q(Z_0(K)) = \inf_{\{\eta:\ \Gamma(\eta,K) \geq C_1\}} Q(z_0), \text{ and}$$

$$F(K) = \sup_{\{\eta:\ \Gamma(\eta,K) \geq C_1\}} \frac{K}{Q(z_0)} = \sup_{\{\eta \geq \eta_{\min}\}} L(K,\eta), \quad (31)$$

where $L(K,\eta) \triangleq K/Q(z_0)$ is a two dimensional function of K and η with $\mathbf{dom}\ L = \{(K,\eta):\ K \geq K_{\min};\ \eta \geq \eta(K)\}$. In the above equation, $\eta_{\min}$ is the threshold corresponding to $K = K_{\min}$. Thus, $F(K)$ can be represented as point-wise supremum of a family of functions and the convexity follows by proving that for each $\eta \geq \eta_{\min}$, $L(K,\eta)$ is a convex function of K, $K \in \mathbf{dom}\ L$ [27]. Differentiating $L(K,\eta)$ twice with respect to K, we get

$$\frac{\partial^2 L}{\partial K^2} = \frac{e^{-z_0^2/2}}{\sqrt{2\pi}Q(z_0)^2}\Big[\frac{3K-2}{(2K-1)^{3/2}} + \frac{K}{2K-1}\Big(\frac{2e^{-z_0^2/2}}{\sqrt{2\pi}Q(z_0)} - z_0\Big)\Big]. \quad (32)$$

For practical values of K $(\geq 1$), the first term is always positive. The second term is always positive for $z_0 < 0$. For $z_0 \geq 0$, we use the upper bound for Q-function [29], with $a = 0.344, b = 5.334$ and get, $[2e^{-z_0^2/2}]/[\sqrt{2\pi}Q(z_0)] - z_0 \geq 2\Big[(1-a)z_0 + a\sqrt{z_0^2+b}\Big] - z_0 \geq (1-a)z_0 \geq 0$. Thus, $L(K,\eta)$ is convex in K and hence $F(K)$ is convex in K.

We now prove the main proposition. From (14), we see that $p(K) = C_2 Q(Z_0(K))$. Using (8), $D_{\text{avg}}(K)$ can be written as $D_{\text{avg}}(K) = \sum_{n=1}^{M}(1/C_2^n)(K+N_S)/Q^n(Z_0)$. Let $G_n(K) \triangleq K/Q^n(Z_0)$ and $H_n(K) \triangleq 1/Q^n(Z_0)$, with $n \geq 1$. The arguments that were used to prove convexity of $K/Q(Z_0)$ hold for $G_n(K)$ and $H_n(K)$ as well, and it can be easily verified that $G_n(K)$ and $H_n(K)$ are convex in K. The convexity of $D_{\text{avg}}(K)$ follows from this, since it can be written as a non-negative weighted sum of convex functions and is therefore convex [27]. ■

REFERENCES

[1] A. Sharma and C. R. Murthy, "A group testing based spectrum hole search using a simple sub-nyquist sampling scheme," in *Proc. Globecom*. 2012, pp. 1–6, IEEE.

[2] D. Du and F. Hwang, *Combinatorial group testing and its applications*, World Scientific, 1993.

[3] S. Haykin, "Cognitive radio: brain-empowered wireless communications," *IEEE J. Sel. Areas Commun.*, vol. 23, no. 2, pp. 201–220, Feb. 2005.

[4] J. Mitola and G. Q. Maguire, Jr., "Cognitive radio: making software radios more personal," *IEEE Personal Commun. Mag.*, vol. 6, no. 4, pp. 13–18, Aug. 1999.

[5] Y. C. Liang, K. C. Chen, G. Y. Li, and P. Mahonen, "Cognitive radio networking and communications: An overview," *IEEE Trans. Veh. Technol.*, vol. 60, no. 7, pp. 3386–3407, Sept. 2011.

[6] D. Cabric, S. M. Mishra, D. Willkomm, R. Brodersen, and A. Wolisz, "A cognitive radio approach for usage of virtual unlicensed spectrum," in *In Proc. of 14th IST Mobile Wireless Communications Summit*, 2005.

[7] FCC, "Et docket no. 02-155," *Spectrum policy task force report*, Nov. 2002.

[8] T. Yucek and H. Arslan, "A survey of spectrum sensing algorithms for cognitive radio applications," *IEEE Commun. Surveys Tuts.*, vol. 11, no. 1, pp. 116–130, 2009.

[9] Y. Zeng, Y. C. Liang, A. T. Hoang, and R. Zhang, "A review on spectrum sensing for cognitive radio: challenges and solutions," *EURASIP J. Adv. Signal Process.*, vol. 2010, Jan. 2010.

[10] E. Axell, G. Leus, E.G. Larsson, and H.V. Poor, "Spectrum sensing for cognitive radio : State-of-the-art and recent advances," *IEEE Signal Process. Mag.*, vol. 29, no. 3, pp. 101–116, 2012.

[11] H. Urkowitz, "Energy detection of unknown deterministic signals," *Proc. IEEE*, vol. 55, no. 4, pp. 523–531, Apr. 1967.

[12] N. C. Beaulieu, W. L. Hopkins, and P. J. McLane, "Interception of frequency-hopped spread-spectrum signals," *IEEE J. Sel. Areas Commun.*, vol. 8, no. 5, pp. 853–870, Jun. 1990.

[13] B. K. Levitt, U. Cheng, A. Polydoros, and M. K. Simon, "Optimum detection of slow frequency-hopped signals," *IEEE Trans. Commun.*, vol. 42, no. 2/3/4, pp. 1990–2000, Feb./Mar./Apr. 1994.

[14] D. Cabric, A. Tkachenko, and R. W. Brodersen, "Experimental study of spectrum sensing based on energy detection and network cooperation," in *ACM TAPAS*, New York, NY, USA, 2006.

[15] L. Luo, N. M. Neihart, S. Roy, and D. J. Allstot, "A two-stage sensing technique for dynamic spectrum access," *IEEE Trans. Wireless Commun.*, vol. 8, no. 6, pp. 3028–3037, 2009.

[16] N. M. Neihart, S. Roy, and D. J. Allstot, "A parallel, multi-resolution sensing technique for multiple antenna cognitive radios," in *ISCAS*, 2007, pp. 2530–2533.

[17] M.F. Hanif, P.J. Smith, D.P. Taylor, and P.A. Martin, "Mimo cognitive radios with antenna selection," *IEEE Trans. Wireless Commun.*, vol. 10, no. 11, pp. 3688–3699, 2011.

[18] Z. Quan, S. Cui, A. H. Sayed, and H. V. Poor, "Optimal multiband joint detection for spectrum sensing in cognitive radio networks," *IEEE Trans. Signal Process.*, vol. 57, no. 3, pp. 1128–1140, Mar. 2009.

[19] P. Paysarvi-Hoseini and N. C. Beaulieu, "Optimal wideband spectrum sensing framework for cognitive radio systems," *IEEE Trans. Signal Process.*, vol. 59, no. 3, pp. 1170–1182, Mar. 2011.

[20] J. Treichler, M. Davenport, and R. Baraniuk, "Application of compressive sensing to the design of wideband signal acquisition receivers," in *Proc. U.S./Australia Joint Work. DASP*, Sept. 2009.

[21] A. V. Oppenheim and R. W. Schafer, *Discrete-time signal processing*, Prentice Hall, 1989.

[22] Z. Quan, S. Cui, H. V. Poor, and A. Sayed, "Collaborative wideband sensing for cognitive radios," *IEEE Signal Process. Mag.*, vol. 25, no. 6, pp. 60–73, Nov. 2008.

[23] P. Wang, J. Fang, N. Han, and H. Li, "Multiantenna-assisted spectrum sensing for cognitive radio," *IEEE Trans. Veh. Technol.*, vol. 59, no. 4, pp. 1791–1800, May 2010.

[24] H. V. Poor, *An introduction to signal detection and estimation*, Springer-Verlag, 1994.

[25] C. Cordeiro, K. Challapali, D. Birru, and Sai Shankar N., "IEEE 802.22: the first worldwide wireless standard based on cognitive radios," in *Proc. DySPAN*, 2005, pp. 328–337.

[26] M. Abramowitz and I. A. Stegun, *Handbook of mathematical functions with formulas, graphs, and mathematical tables*, Dover Publications, 1964.

[27] S. Boyd and L. Vandenberghe, *Convex Optimization*, Cambridge University Press, Mar. 2004.

[28] Y. C. Liang, Y. Zeng, E. C. Y. Peh, and A. T. Hoang, "Sensing-throughput tradeoff for cognitive radio networks," *IEEE Trans. Wireless Commun.*, vol. 7, no. 4, pp. 1326–1337, 2008.

[29] P. Borjesson and C.-E. Sundberg, "Simple approximations of the error function q(x) for communications applications," *IEEE Trans. Commun.*, vol. 27, no. 3, pp. 639–643, Mar. 1979.

Abhay Sharma received the B.E. (Hons) Electrical and Electronics Engineering degree from BITS, Pilani, India, in 1996 and the M.S. degree in Electrical Engineering from Ohio State University, Columbus, in 2000. From 2000 to 2005 he worked with Analog Devices Inc., where he designed and implemented physical layer algorithms for cellular communication. From 2006 to 2009 he worked with Allgo Embedded Systems, Bangalore, India, in the area of video signal processing and emerging W-PAN wireless technologies. He is currently pursuing his Ph.D. in Electrical Communication Engineering at the Indian Institute of Science, Bangalore, India. His research interests include sparse signal processing, wireless communications, statistical signal processing and machine learning.

Chandra R. Murthy (S'03–M'06–SM'11) received the B.Tech. degree in Electrical Engineering from the Indian Institute of Technology, Madras in 1998, the M.S. and Ph.D. degrees in Electrical and Computer Engineering from Purdue University and the University of California, San Diego, in 2000 and 2006, respectively.

From 2000 to 2002, he worked as an engineer for Qualcomm Inc., where he worked on WCDMA baseband transceiver design and 802.11b baseband receivers. From Aug. 2006 to Aug. 2007, he worked as a staff engineer at Beceem Communications Inc. on advanced receiver architectures for the 802.16e Mobile WiMAX standard. In Sept. 2007, he joined as an assistant professor at the Department of Electrical Communication Engineering at the Indian Institute of Science, where he is currently working. His research interests are in the areas of Cognitive Radio, Energy Harvesting Wireless Sensors and MIMO systems with channel-state feedback. He is currently serving as an associate editor for the IEEE Signal Processing Letters and as an elected member of the IEEE SPCOM Technical Committee for the years 2014-16.